Sandpile Model with Tokamaklike Enhanced Confinement Phenomenology

S. C. Chapman,[1,*] R. O. Dendy,[2] and B. Hnat[1]

[1]*Physics Department, University of Warwick, Coventry CV4 7AL, United Kingdom*

[2]*EURATOM/UKAEA Fusion Association, Culham Science Centre, Abingdon, Oxfordshire OX14 3DB, United Kingdom*

(Received 12 October 2000)

Confinement phenomenology characteristic of magnetically confined plasmas emerges naturally from a simple sandpile algorithm when the parameter controlling redistribution scale length is varied. Close analogs are found for enhanced confinement, edge pedestals, and edge localized modes (ELMs), and for the qualitative correlations between them. These results suggest that tokamak observations of avalanching transport are deeply linked to the existence of enhanced confinement and ELMs.

DOI: 10.1103/PhysRevLett.86.2814 PACS numbers: 52.55.Dy, 45.70.Ht, 52.35.Ra, 52.55.Fa

The introduction of the sandpile paradigm [1–3] into magnetized plasma physics (fusion [4–12], magnetospheric [13–15], and accretion disk [16–18]: for recent reviews see Refs. [19,20]) has opened new conceptual avenues. It provides a framework within which observations of rapid nondiffusive nonlocal transport phenomena can be studied; recent examples include analyses of auroral energy deposition derived from global imaging [15], and of electron temperature fluctuations in the DIII-D tokamak [12], both of which involve avalanching. Insofar as such phenomena resemble those in experimental sandpiles or mathematically idealized models thereof, they suggest that the confinement physics of macroscopic systems (plasma and other) may reflect unifying underlying principles.

In this paper we present results suggesting that this unity may extend to some of the most distinctive features of toroidal magnetic plasma confinement: enhanced confinement regimes ("H modes"), edge localized modes ("ELMs"), steep edge gradients ("edge pedestal"), and their observed phenomenological and statistical correlations — for recent quantitative studies, see, for example, Refs. [21–23] and references therein. An important question is whether the L to H transition necessarily reflects a catastrophic bifurcation of confinement properties or can be associated with a monotonic change in the character of the turbulence [23]. Transitional behavior resembling that observed in fusion plasmas has been found in other sandpile algorithms: for example, in Ref. [4] a local sheared flow region is imposed which reduces the characteristic avalanche length thereby affecting confinement, and in Ref. [6], changes in the redistribution rule lead to changes in profile stiffness. We show that key elements of the observed phenomenology emerge naturally from a simple one-dimensional sandpile model, that of Chapman [24], which incorporates other established models [1,25] as limiting cases. This centrally fueled (at cell $n = 1$) model's distinctive algorithmic feature relates to the local redistribution of sand at a cell (say, at $n = k$) where the critical gradient z_c is exceeded: the sandpile is instantaneously flattened behind the unstable cell over a length L_f, embracing the cells $n = k - (L_f - 1), k - (L_f - 2), \ldots, k$; and this sand is conservatively relocated to the cell at $n = k + 1$. L_f defines the length scale over which the most rapid redistribution occurs; in a plasma context this could be considered a proxy for turbulent correlation length or eddy size. In Ref. [24] the sandpile is explored for all regimes $1 < L_f < N$ for both constant and fluctuating critical gradient z_c. Here we consider the dynamics of the more realistic case with random fluctuations in z_c; the system is robust in that once fluctuations are introduced in the critical gradient, the behavior is essentially insensitive to both their level and spectral properties [24]; see also Ref. [19]. The limit $L_f = 1$ is the fixed point corresponding to the centrally fueled algorithm of Ref. [1] in one dimension. In the limit $L_f = N$ (where N is the number of cells in the sandpile) the sandpile is flattened everywhere behind an unstable cell as in Refs. [19,25]. A real space renormalization group approach [26] shows that the robust scale free dynamics for the limiting case $L_f = N$ corresponds to a nontrivial (repulsive) fixed point (see, e.g., Ref. [3]). The essential result of Ref. [24] is that different regimes of avalanche statistics emerge, resembling a transition from regular to intermittent dynamics reminiscent of deterministic chaos. The control parameter is the normalized redistribution scale length L_f/N which specifies whether the system is close to the nontrivial $L_f = N$ fixed point.

Height profiles for the sandpile with 512 cells, time averaged over many thousands of avalanches, are shown in Fig. 1 for three different values of the fluidization length L_f in the range $50 < L_f < 250$. The sandpile profile shape, stored gravitational potential energy, and edge structure (smooth decline or pedestal) correlate with each other and with L_f. As L_f is reduced, the edge pedestal steepens and the time averaged stored energy rises; multiple "barriers" (regions of steep gradient) are visible in trace (a) and to some extent trace (b) of Fig. 1. Time evolution of the sandpile for $L_f = 50$, 150, and 250, respectively, is quantified in Figs. 2–4. The top traces show total stored energy, the middle traces show the position of the edge of the sandpile (the last occupied cell), and the bottom traces show the magnitude and occurrence times of mass loss events (hereafter MLEs) in which sand is lost from the system by being transferred beyond the 512th cell. Time

 0031-9007/01/86(13)/2814(4)$15.00

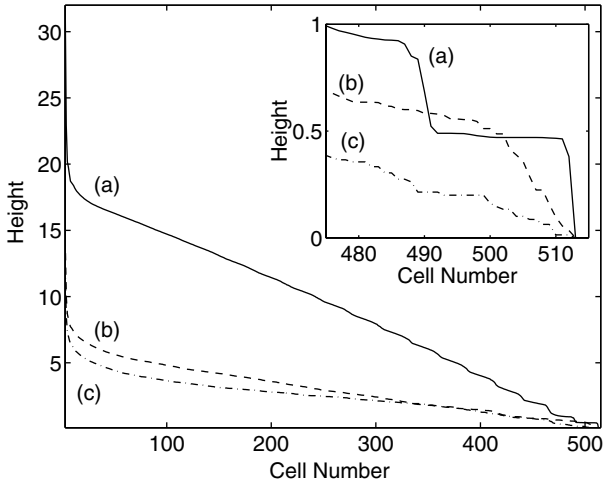

FIG. 1. Time averaged height profiles of the 512 cell sandpile for $L_f = (a)50$, $(b)150$, and $(c)250$. Inset: edge structure.

is normalized to the mean interavalanche time $\Delta\tau$ (proportional to the fueling rate). The sandpile is fueled only at the first cell, so that the great majority of avalanches terminate before reaching the 512th cell (these are classified as internal). While internal avalanches result in energy dissipation (recorded in the upper traces of Figs. 2–4), and may alter the position of the edge of the sandpile, they do not result in an MLE; there are corresponding periods of quiescence in the middle and lower traces of Figs. 2–4. Conversely the MLEs are associated with sudden inward movement of the sandpile edge, and in this important sense appear to be edge localized. However, MLEs and the associated inward edge movement are, in fact, the result of systemwide avalanches triggered at the sandpile center (cell $n = 1$). The character of the MLEs changes with L_f. In Fig. 2, where the mean and peak stored energy are greatest, the MLEs are similar to each other and occur with some regularity. The regularity of MLE occurrence in Fig. 3 is less marked, the magnitude of the largest MLEs is greater than in Fig. 2, and there is greater spread in MLE size. This trend continues in Fig. 4, which also has the lowest stored energy. These effects correlate with the underlying dynamics of the sandpile. Figure 5 plots the relation between average stored energy and L_f for the $N = 512$ system and much larger $N = 4096$ and 8192 systems (normalized to the system size N). The curves coincide, demonstrating invariance with respect to system size, with an inverse power law with slope close to -2 for $L_f/N < 1/4$, and a break at $L_f/N \sim 1/4$. These two regimes yield the quasiregular and quasi-intermittent dynamics in Figs. 2–4 (see also the plot of avalanche length distribution against L_f in Fig. 8 of Ref. [24]). The parameter L_f/N is a measure of proximity of this high dimensional system to the $L_f = N$ nontrivial fixed point. This determines both the apparent complexity of the time series in Figs. 2–4 and the underlying statistical simplicity described below, which is also invariant with respect to system size.

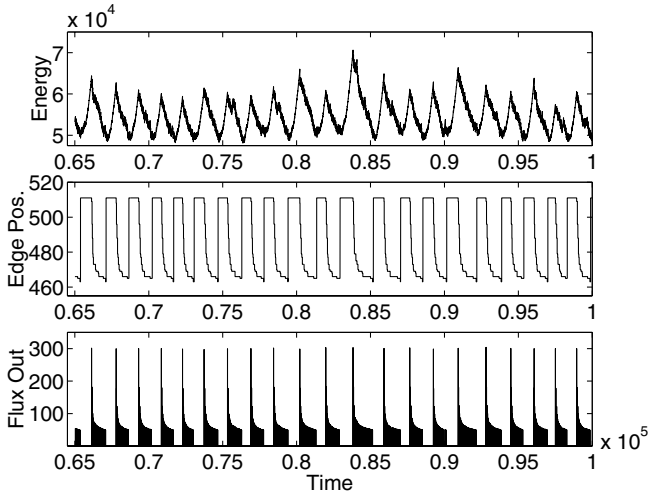

FIG. 2. Time evolution of the 512 cell sandpile with $L_f = 50$: (top) stored energy; (middle) position of last occupied cell; (lower) magnitude and occurrence of mass loss events.

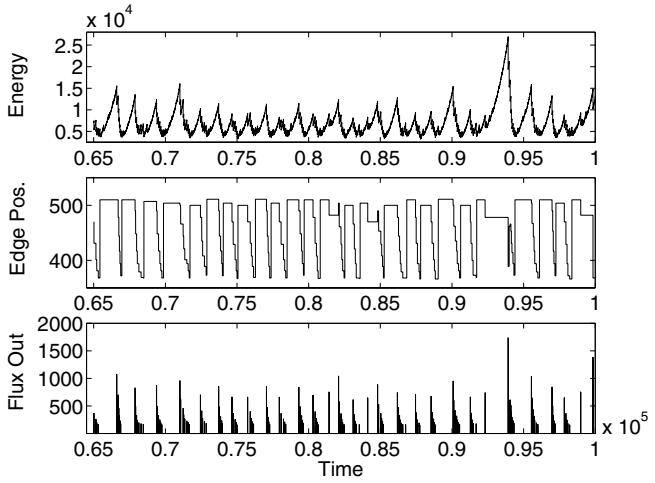

FIG. 3. As Fig. 2, for $L_f = 150$.

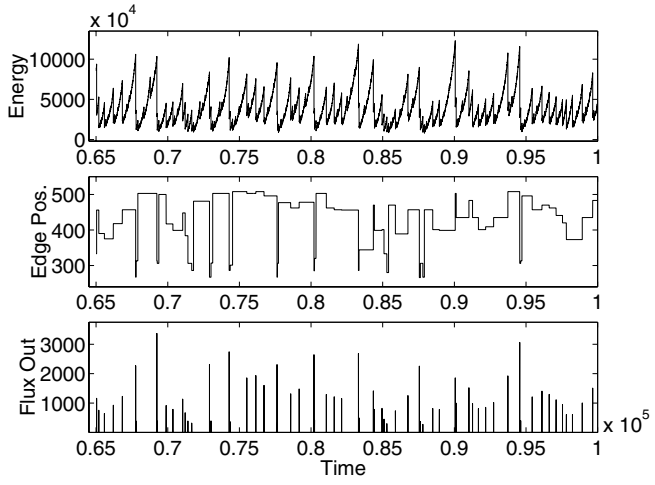

FIG. 4. As Fig. 2, for $L_f = 250$.

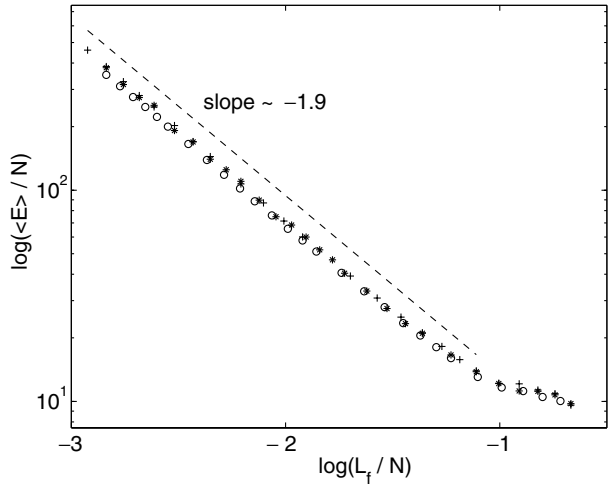

FIG. 5. Average stored energy versus L_f/N for sandpiles of $N = 512$, 4096, and 8192. Energy is normalized to the $L_f = 1$ case (effectively to N^2).

There is systematic correlation between time averaged stored energy $\langle E \rangle$ and MLE frequency f_{MLE}, as shown in Fig. 6. To obtain these curves, which are again normalized to system size, we have derived MLE frequencies using a standard algorithm previously used [22] to assign frequencies to ELMs observed in tokamak plasmas in the Joint European Torus (JET). Since the sandpile often generates bursts of mass loss with structure down to the smallest time scales, which might not be resolvable under experimental conditions, we have followed Ref. [22] in applying a (relatively narrow) measurement window of width $450\Delta\tau$ to obtain f_{MLE}. The correlation between $\langle E \rangle$ and f_{MLE} is a noteworthy emergent property; furthermore, Fig. 6's characteristic curve is very similar to that of Fig. 6 of Ref. [21], which relates measured energy confinement to ELM frequency in JET. Energy confinement time τ_c can be defined for the sandpile by dividing the time averaged stored energy $\langle E \rangle$ by the time averaged energy dissipation rate $\langle \Delta E \rangle$ (where ΔE is the energy dissipated in a single avalanche). The embedded plot of Fig. 6 shows τ_c against MLE frequency f_{MLE}.

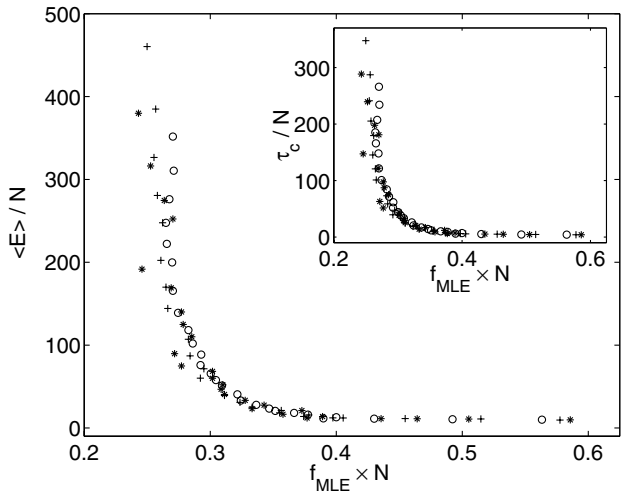

FIG. 6. Average stored energy versus MLE frequency, and (inset) τ_c versus MLE frequency for sandpiles of $N = 512$, 4096, and 8192. Energy and MLE frequency are normalized as in Fig. 5.

Finally, we explore the situation where there is a secular change in the redistribution algorithm: in Fig. 7, L_f decreases slowly, continuously, and linearly with time, from one constant value to another over a period encompassing many tens of thousands of avalanches. There is a corresponding time evolution of the energy confinement properties of the sandpile and of the character of the MLEs. Figure 7 (top) shows total stored energy as a function of time as L_f changes from 250 at $t = 4 \times 10^4$ to 50 at $t = 1.15 \times 10^5$, while $\sim 10^5$ avalanches occur: over a period of time corresponding to a few tens of MLEs, the system smoothly evolves from low to high confinement. This is accompanied by a gradual change in character of the time variation in the sandpile edge [position of last occupied cell, Fig. 7 (middle)] and of the MLEs [Fig. 7 (lower)], from large amplitude to small and from irregular to regular. Figure 7 can perhaps be regarded as this sandpile's analog of, for example, Fig. 2 of Ref. [22] or Fig. 2 of Ref. [23]. The essential point here is that the sandpile apparently freely explores phase space with changing control parameter L_f/N. Characteristic properties of the dynamics (whether quasiregular or quasi-intermittent) and, correspondingly, confinement properties (such as stored energy and MLE characteristics) smoothly follow changes in this parameter rather than exhibiting a sudden phase transition or catastrophe.

By varying a single control parameter in the sandpile algorithm, we have shown correlations between stored energy, confinement times, sandpile profile, sandpile edge structure, and the amplitude, frequency, and dynamical character of mass loss events. We have also seen how slow secular change in the control parameter produces a smooth

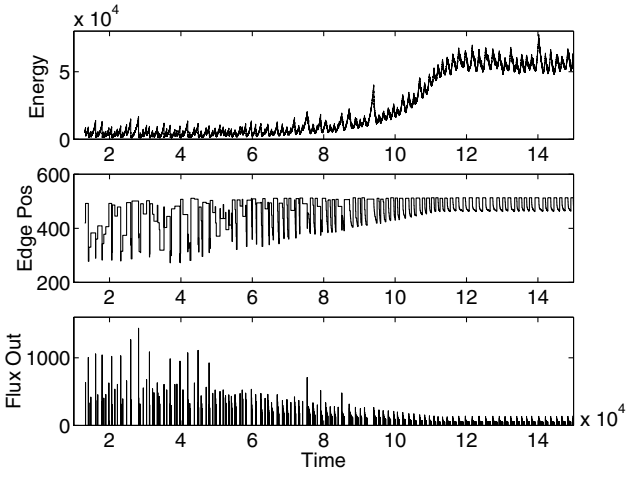

FIG. 7. Time evolution of (top) stored energy, (middle) sandpile edge position, and (lower) MLEs, as L_f changes slowly and linearly from 250 to 50.

evolution in confinement properties. If a single control parameter analogous to L_f/N exists for tokamaks, it can in principle be found from experimental data by examining scaling with respect to system size as above.

The existence of such extensive tokamaklike phenomenology, emergent from a very simple system, is a novel discovery. Insofar as the phenomenological resemblance is close, there is more to be learned. A minimalist interpretation starts from the premise that the sandpile algorithm of Ref. [24] provides a simple one-parameter model for studying generic nonlocal transport, conditioned by a critical gradient, in a macroscopic confinement system. Changing the value of the single control parameter L_f then corresponds to altering the range in configuration space over which the transport process operates. It then follows from the results in the present paper that this may be the minimum requirement to generate those aspects of tokamaklike confinement phenomenology described. This is a significant conclusion, but one can consider a more far-reaching one. A possible maximalist interpretation attaches greater weight to recent observations [8,11,12] of avalanching transport in tokamaks and in large scale numerical simulations [9,10] thereof, and therefore regards the avalanching transport that is built into sandpile algorithms as an additional point of contact with magnetically confined plasmas. One would then infer from the present results that tokamak observations of avalanching transport are deeply linked to the existence of enhanced confinement and ELMs.

We are grateful to Jack Connor, George Rowlands, David Ward, and Nick Watkins for comments and suggestions. S. C. C. was supported by a PPARC lecturer fellowship, R. O. D. by Euratom and the UK DTI, and B. H. by HEFCE.

*Email address: sandrac@astro.warwick.ac.uk

[1] P. Bak, C. Tang, and K. Wiesenfeld, Phys. Rev. Lett. **59**, 381 (1987).
[2] P. Bak, C. Tang, and K. Wiesenfeld, Phys. Rev. A **38**, 364 (1988).
[3] H. J. Jensen, *Self-Organised Criticality: Emergent Complex Behaviour in Physical and Biological Systems* (Cambridge University Press, Cambridge, U.K., 1998).
[4] D. E. Newman, B. A. Carreras, P. H. Diamond, and T. S. Hahm, Phys. Plasmas **3**, 1858 (1996).
[5] B. A. Carreras, D. Newman, V. E. Lynch, and P. H. Diamond, Phys. Plasmas **3**, 2903 (1996).
[6] B. A. Carreras, V. E. Lynch, P. H. Diamond, and M. Medvedev, Phys. Plasmas **5**, 1206 (1998).
[7] R. O. Dendy and P. Helander, Plasma Phys. Controlled Fusion **39**, 1947 (1997).
[8] B. A. Carreras *et al.,* Phys. Rev. Lett. **80**, 4438 (1998).
[9] X. Garbet and R. Waltz, Phys. Plasmas **5**, 2836 (1998).
[10] Y. Sarazin and P. Ghendrih, Phys. Plasmas **5**, 4214 (1998).
[11] T. L. Rhodes *et al.,* Phys. Lett. A **253**, 181 (1999).
[12] P. A. Politzer, Phys. Rev. Lett. **84**, 1192 (2000).
[13] T. S. Chang, IEEE Trans. Plasma Sci. **20**, 691 (1992).
[14] S. C. Chapman, N. W. Watkins, R. O. Dendy, P. Helander, and G. Rowlands, Geophys. Res. Lett. **25**, 2397 (1998).
[15] A. T. Y. Lui *et al.,* Geophys. Res. Lett. **27**, 2397 (2000).
[16] S. Mineshige, M. Takeuchi, and H. Nishimori, Astrophys. J. **435**, L125 (1994).
[17] K. M. Leighly and P. T. O'Brien, Astrophys. J. **481**, L15 (1997).
[18] R. O. Dendy, P. Helander, and M. Tagger, Astron. Astrophys. **337**, 962 (1998).
[19] S. C. Chapman, R. O. Dendy, and G. Rowlands, Phys. Plasmas **6**, 4169 (1999).
[20] S. C. Chapman and N. W. Watkins, Space Sci. Rev. **25**, 293 (2001).
[21] G. M. Fishpool, Nucl. Fusion **38**, 1373 (1998).
[22] W. Zhang, B. J. D. Tubbing, and D. Ward, Plasma Phys. Controlled Fusion **40**, 335 (1998).
[23] J. Hugill, Plasma Phys. Controlled Fusion **42**, R75 (2000).
[24] S. C. Chapman, Phys. Rev. E **62**, 1905 (2000).
[25] R. O. Dendy and P. Helander, Phys. Rev. E **57**, 3641 (1998).
[26] S. W. Y. Tam, T. S. Chang, S. C. Chapman, and N. W. Watkins, Geophys. Res. Lett. **27**, 1367 (2000).